

# Constraints on Glacial Isostatic Adjustment (GIA) Motion in North American Using GPS

G. F. Sella<sup>1</sup>, S. Stein<sup>2</sup>, T. H. Dixon<sup>3</sup>, M. Craymer<sup>4</sup>, T. James<sup>5</sup>, S. Mazzotti<sup>5</sup>, and R. K. Dokka<sup>6</sup>

<sup>1</sup>National Geodetic Survey, NOAA, Silver Spring, MD, USA, giovanni.sella@noaa.gov, <sup>2</sup>Dept. of Geological Sciences, Northwestern University, Evanston, IL, USA, <sup>3</sup>Rosenstiel School of Marine and Atmospheric Science, University of Miami, Miami, FL, USA, <sup>4</sup>Geodetic Survey Division, Natural Resources Canada, Ottawa, ON, Canada, <sup>5</sup>Geological Survey of Canada, Natural Resources Canada, Sidney, BC, Canada, <sup>6</sup>Dept. of Civil & Environmental Engineering and Center for Geoinformatics, Louisiana State University, Baton Rouge, LA, USA

A clear and consistent pattern is seen in both the observed vertical and residual horizontal velocity fields and that is consistent with being caused by GIA.

## Abstract

We use Global Positioning System (GPS) data to measure the motion caused by glacial isostatic adjustment (GIA) due to glacial unloading in eastern North America. The large vertical signal due to GIA (~10mm/yr) in the area of maximum uplift, near Hudson Bay, permits this motion to be resolved with both continuous GPS (CGPS) data and even with episodic GPS (EGPS) data. We present data from 239 CGPS sites throughout North America and 123 EGPS sites of the Canadian Base Network (CBN). We detect a coherent pattern of vertical motions around the area of maximum glacial loading, Hudson Bay. The observed velocities are initially large and upward, and decrease southward from Hudson Bay to zero, delineating the hinge line near the Great Lakes. The position of the hinge line is in agreement with some numerical GIA predictions. The horizontal residual velocities after removing the motion of the rigid North American plate also show a consistent, but more complex pattern than the vertical velocities. In particular we observe larger than expected motions on the east side of the Canadian Rocky Mountains, possibly reflecting larger ice loads and/or changes in mantle viscosity. We believe that this velocity field provides a comprehensive direct description of GIA motion and can be used to constrain GIA model predictions.

## Data Sets

We selected 239 CGPS sites (Figure 1) on the stable interior of North America using standard geologic and seismological criteria: sites are >100 km away from any significant seismicity to avoid any seismic cycle effects and away from any seismogenic faults or active tectonic geomorphic features. Thus we use sites east of the Rocky Mountains and Rio Grande Rift, and exclude sites near Memphis, Tennessee and Charleston, South Carolina, both associated with large magnitude earth-quakes. We also exclude sites along the Northern Gulf of Mexico coast that may be affected by sediment loading, sediment compaction, and slippage along normal faults. For the CGPS sites we analyzed all available data from 1993 to 2006. In addition we analyzed 123 EGPS sites that are part of the Canadian Base Network (CBN). These sites have been occupied for 2-5 days every two to three years from 1994 to 2002.

## Figure 1. Distribution of GPS sites used in this study.

Black diamonds are 124 CGPS sites used to define the motion of rigid North America. Red circles are 115 CGPS sites that may be subject to significant GIA motion. Green diamonds are 123 EGPS sites that are part of the Canadian Base Network (CBN) that are mostly subjected to GIA motion. Note the limited number of sites in the area in and around Hudson Bay where GIA motion is thought to be greatest.



## Method

We use GPSY/OASIS II, Release 5.0 software developed at the Jet Propulsion Laboratory. Offset parameters are estimated at the date of each change of antenna height or model or dome model. Daily position estimates are generated with loose constraints, and then transformed to IGB00. Velocity estimates are based on a weighted least squares line fit to the daily position estimates, including the offset parameters described above. Our velocity error estimates account for white (uncorrelated) and colored (time-correlated) noise and random walk noise following Mao et al. [1999]. We exploit the correlation between WRMS (the weighted root mean square scatter of the daily position estimates about a best fit straight line) and white and flicker noise amplitudes observed in the data of Mao et al. [1999], as outlined in Dixon et al. [2000]. A cubic spline was fit to the IGB00 vertical velocities, and then we identified the regional zero velocity line (hinge line) (Figure 2 Left). We conservatively interpret that sites north and within ~200 km south of this line may be significantly affected by GIA (sites with red arrows). We invert the site velocity data to derive best-fit angular velocity for the plate, minimizing the weighted, least squares misfit to the data, as described by Ward [1990]. Applying our error model to our data set of 124 site velocities yields a  $\chi^2$  per degree of freedom ( $\chi^2_\nu$ ) of 1.0 for the rigid plate model, close to the expected value of 1.0. This suggests that our error model is reasonable and that the region sampled by these data can be assumed rigid within data uncertainty. If we include the 115 CGPS sites that may be significantly affected by GIA, 239 site solution, gives a larger  $\chi^2_\nu = 1.5$  suggesting that the plate can no longer be assumed to be rigid. We obtain an angular velocity for North America that is very similar to other recent studies:

Lat	Lon	Omega [°/y]	Author(s)	Number of sites frame
-5.67 N	-84.75 E	0.196	Sella et al., 2007	124 sites IGB00
-7.37 N	-84.36 E	0.188	SNARF 1.0	
-2.7 N	-84.6 E	0.202	Calais et al., 2006	119 sites ITRF2000
-5.04 N	-83.14 E	0.194	Allamimi et al., 2002	ITRF2000
-2.39 N	-79.08 E	0.199	Sella et al. 2002	68 sites ITRF97

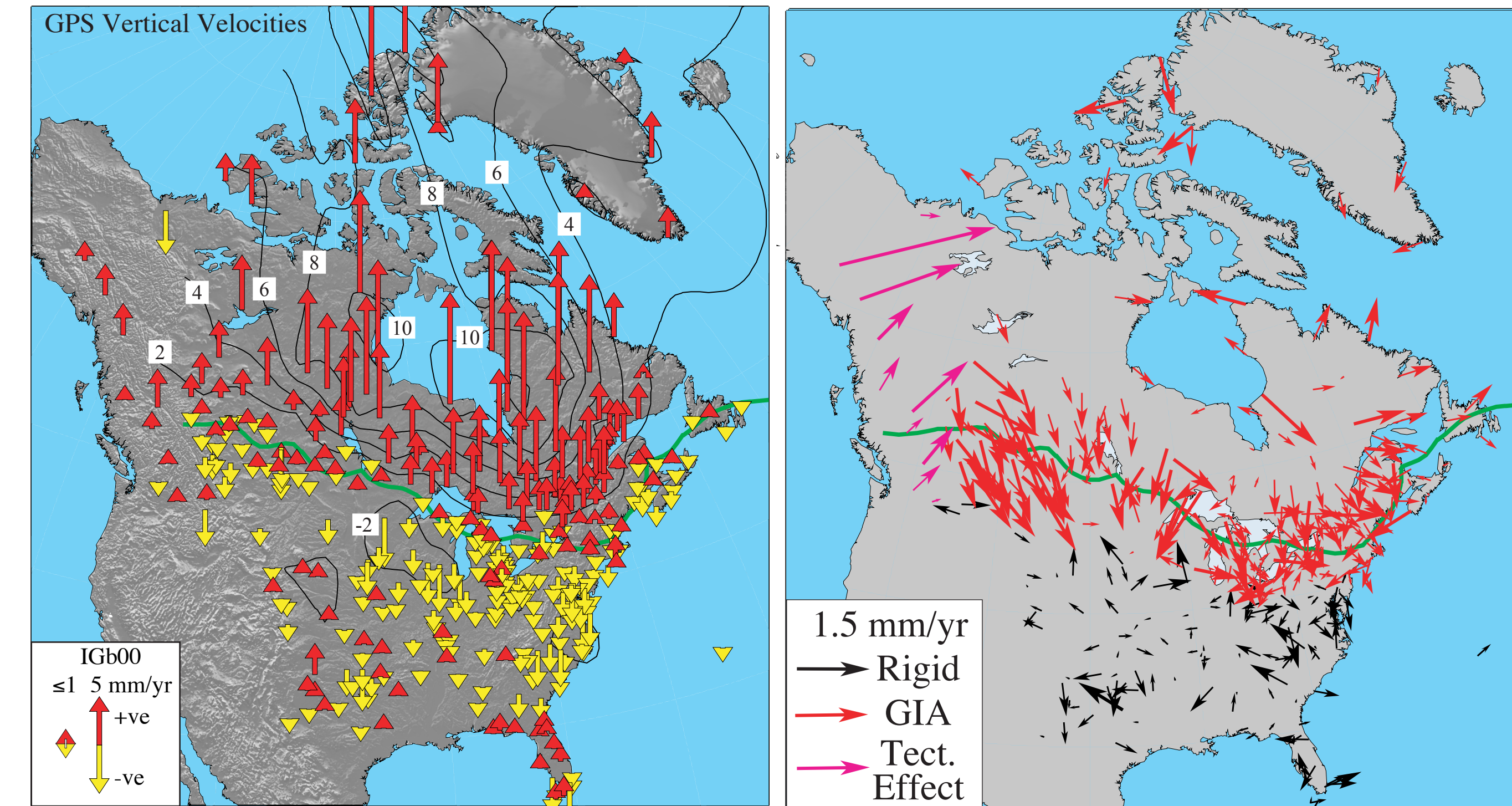
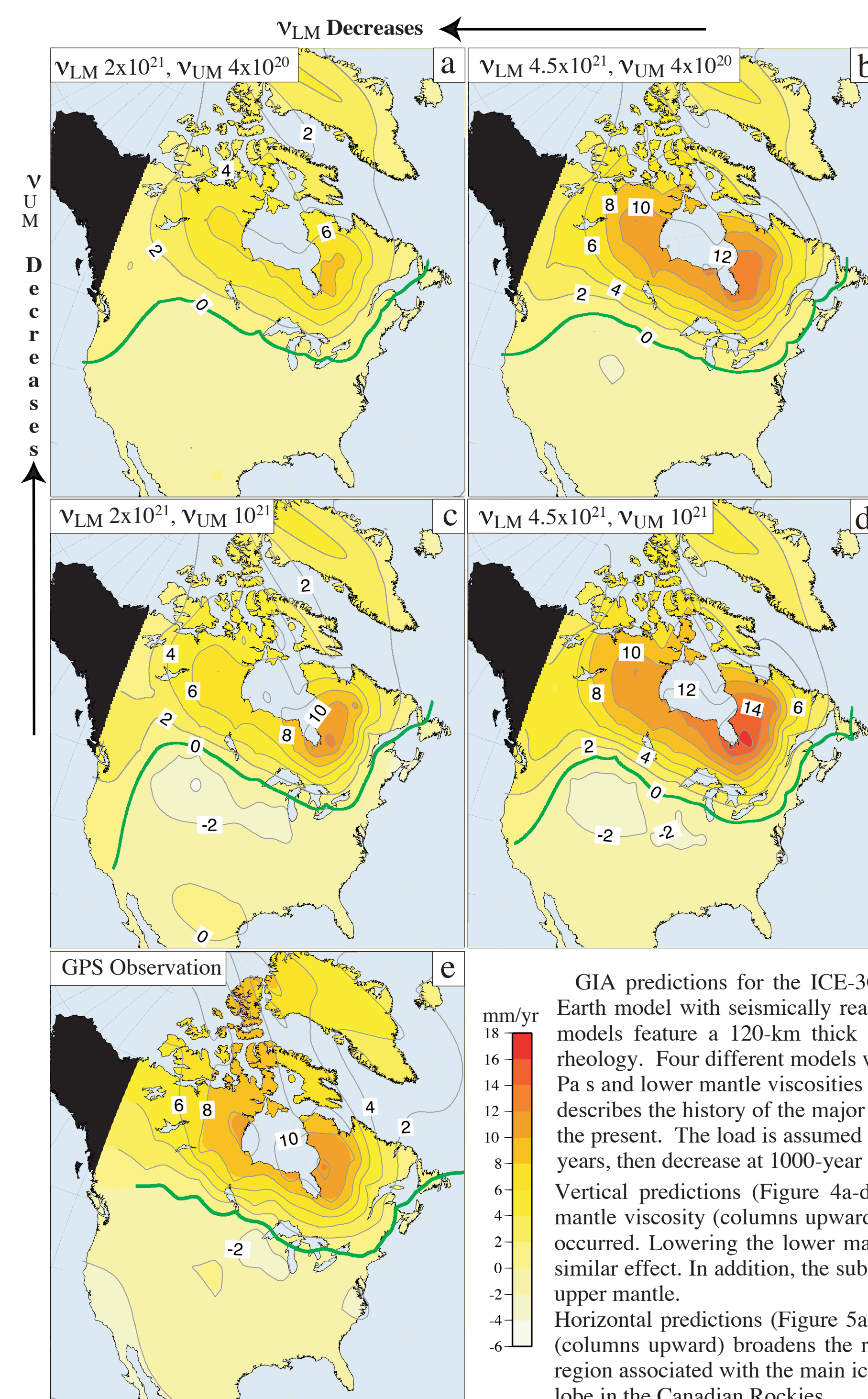


Figure 2. Left: Vertical GPS site motions with respect to IGB00. Green line shows interpolated "hinge line" separating uplift from subsidence. Right: Horizontal motion site residuals after subtracting best fit rigid plate rotation model defined by sites shown with black arrows. Red vectors represent sites primarily affected by GIA. Purple vectors represent sites that include tectonic effects.



## Figure 4 (left).

Comparison of predicted vertical motion for four different viscosity structures (a-d). The predicted motions for each model match the GPS data (e) well. Green line is interpolated hinge line 0 mm/yr.

## Figure 5 (right).

Comparison of predicted horizontal motion for four different viscosity structures (a-d). The predicted motions differ significantly, and none fit the GPS data (e) well. Green line is interpolated hinge line 0 mm/yr.

## GIA Models

GIA predictions for the ICE-3G loading history were generated assuming a laterally homogeneous Earth model with seismically realistic depth-varying density and elastic parameter profiles. The Earth models feature a 120-km thick elastic lithosphere and a mantle with a linear Maxwell viscoelastic rheology. Four different models with upper mantle (120 to 670 km depth) viscosities of  $4 \times 10^{20}$  and  $10^{21}$  Pa s and lower mantle viscosities of  $2 \times 10^{21}$  and  $4.5 \times 10^{21}$  Pa s were run. The ICE-3G ice sheet history describes the history of the major global ice complexes ice sheet, from Last Glacial Maximum (LGM) to the present. The load is assumed to linearly increase from nil at 100,000 years to its maximum at 18,000 years, then decrease at 1000-year increments.

Vertical predictions (Figure 4a-d) show that lowering the upper mantle viscosity for constant lower mantle viscosity (columns upwards) decreases the uplift rate, because more of the relaxation has already occurred. Lowering the lower mantle viscosity for constant upper mantle viscosity rows leftward has a similar effect. In addition, the subsidence in the forebulge area decreases for lower viscosity values in the upper mantle.

Horizontal predictions (Figure 5a-d) vary even more dramatically. Lowering the upper mantle viscosity (columns upward) broadens the region of outward motion and speeds it up. The broader outward flow region associated with the main ice sheet centered on Hudson Bay overwhelms the effect of the secondary lobe in the Canadian Rockies.

## Observed GPS Velocities

The vertical velocities (far left) show fast rebound (~10mm/yr) near Hudson Bay, the site of thickest ice at the last glacial maximum, which changes to slower subsidence (1-2 mm/yr) south of the Great Lakes. This pattern is illustrated by the "hinge line" separating uplift from subsidence, which is consistent with water level gauges along the Great Lakes. In addition two lobes of high uplift rate east and northwest of Hudson Bay appear to correspond with two lobes of maximum ice thickness proposed in ICE-5G (Peltier, 1998) (See Figure 6).

The horizontal velocities are more scattered but show motions directed outward from Hudson Bay and secondary ice maxima in western Canada (Figure 2 right and 3). In addition, the motions show a pattern of south-southeast directed flow in southwestern Canada. Some of the horizontal scatter is presumably a combination of local site effects and intraplate tectonic signal, but the pattern in the far field (beyond the GIA) is not clear.

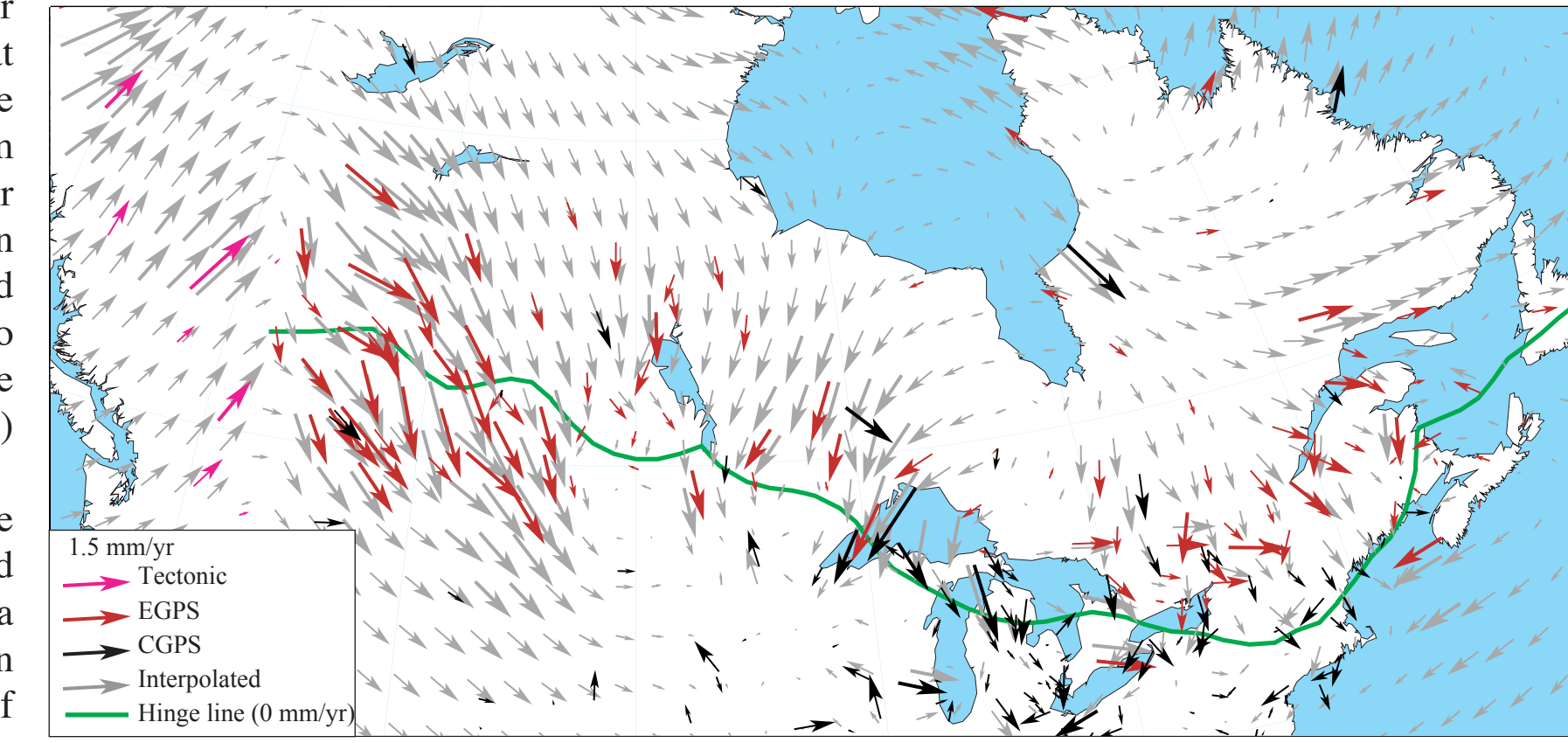


Figure 3. GPS horizontal velocities with motion of rigid North America removed. Interpolated velocity field based on these data are shown in light grey. [Smith and Wessel, 1990; Wessel and Smith, 1998].

## GIA Models and Observations Compared

Perhaps the most striking aspect of the model variations (Figure 4 and 5) is the fact that different viscosity models better fit the vertical (Figure 4d and e) and horizontal data (Figure 5c and e), similar to the results of Argus et al. (1999). The major reasons for model misfit are uncertainties associated with the ice load history, and the assumption of laterally homogeneous rheology. Figure 5 shows the effect of a larger ice load west of Hudson Bay, as now included in the newer ICE-5G model [Peltier, 2004]. Although our attempt to mimic ICE-5G is coarse and the available GPS data is limited comparing Figures 6b and 5e is very encouraging. The misfits between the observed GPS data and the significant variations between GIA models illustrate the potential of GPS data for improving GIA models.

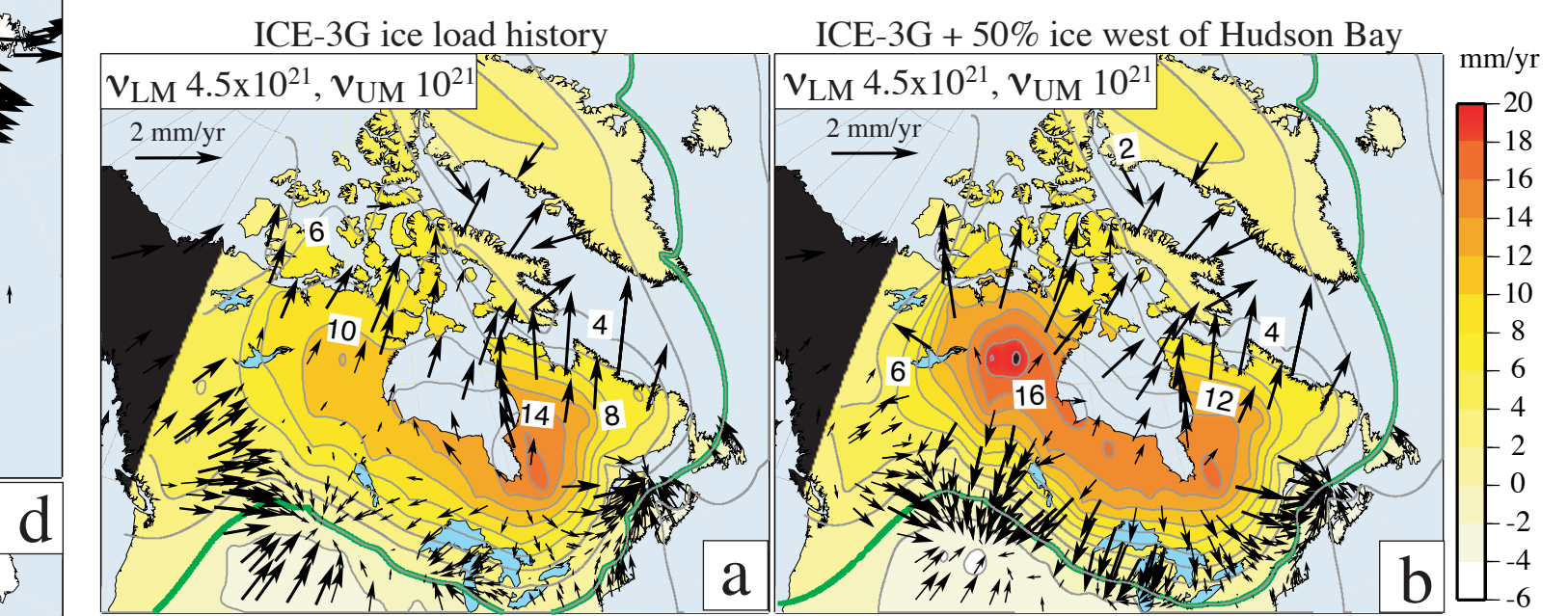


Figure 6. Predicted vertical (color coded contours) and horizontal (arrows) motion for ICE-3G ice load (left) and that load with additional ice west of Hudson Bay (right). The predicted motions differ significantly and would be resolvable with additional GPS data. Green line is interpolated hinge line 0 mm/yr.

## Conclusions

Observed GPS vertical velocities (Figure 2) show a very distinctive oval shaped bulls eye centered in Hudson Bay, the area of maximum ice loading, and have magnitudes of >10 mm/yr. This pattern agrees closely with that predicted by GIA model predictions.

Residual horizontal velocities after removing North America plate motion show a complicated but recognizable pattern of velocities (Figure 2 and 3) that are consistent with our GIA model predictions (Figure 4 and 5).

Discriminating between our GIA models using our GPS data is not unequivocal. This may reflect a number of different factors including:

GPS residual velocities still contain non-GIA related motion that is local and/or regional in origin.

Our GIA models vertical viscosity profile may not be optimal and does not account for well recognized lateral variations in mantle viscosity.

The ice loading history we used may be inaccurate over certain time periods and/or some parts of the ice sheet and is based largely on relative sea level obtained near coastlines, and hence much of the southern margin of the Laurentide ice sheets are poorly constrained.

Additional information and GPS data tables are available in

Sella, Stein, Dixon, Craymer, James, Mazzotti, and Dokka, 2007. Observations of glacial isostatic adjustment in "stable" North America with GPS, 2007. Geophysical research Letters, vol 34, L02306, doi:10.1029/2006GL027081.